Supporting Information

Charge Transport Across Insulating Self-Assembled Monolayers: Non-Equilibrium Approaches and Modeling to Relate Current and Molecular Structure

Fatemeh Mirjani,[*,†] Joseph M. Thijssen,[‡] George M. Whitesides,[¶] and Mark A. Ratner[§]

E-mail: fateme.mirjani@gmail.com

[*]To whom correspondence should be addressed

[†]Chemical Engineering Department, Delft University of Technology, Julianalaan 136, 2628 BL Delft, The Netherlands

[‡]Kavli Institute of Nanoscience, Delft University of Technology, Lorentzweg 1, 2628 CJ Delft, The Netherlands

[¶]Department of Chemistry and Chemical Biology, Harvard University, 12 Oxford, Cambridge, Massachusetts, 02138, USA; and Kavli Institute for Bionano Science and Technology, Harvard University, 29 Oxford, Cambridge, Massachusetts, 02138, USA

[§]Department of Chemistry and Non-Equilibrium Research Center, Northwestern University, 2145 Sheridan Road, Evanston, Illinois, 60208-3113, USA

Determination of the Tight Binding Parameters

In this section we present the procedure for finding the parameters of the TBTM in some detail. We start with the formal description of the model.

The probability for electron tunneling is low enough to neglect two electrons tunneling at the same time, and we can safely neglect spin. This junction is then represented by a simple, essentially linear tight-binding system, coupled to two non-interacting semi-infinite leads. The (extended Hückel-like) Hamiltonian[1] of the molecular region reads

$$H_{\text{molecule}} = -\sum_{\substack{i,j \\ i<j}} t_{i,j}[d_i^\dagger d_j + \text{H.c.}] + \sum_{i=1}^{N} \varepsilon_i d_i^\dagger d_i \tag{1}$$

where H.c. denotes the Hermitian conjugate and N is the length of the interacting chain. The parameters $t_{i,j}$ represent the tunneling amplitudes between the atomic orbitals ϕ_i and ϕ_j within the molecule. The electron creation and annihilation operators, $d_i^\dagger$ and d_j satisfy the usual anti-commutation relations. The second term in the Hamiltonian represents the site energies ε_i.

The Schrödinger equation then takes the form $\text{HC}_\alpha = E_\alpha \text{SC}_\alpha$ where C_α is a vector with coefficients corresponding to ϕ_i such that the molecular orbital $\psi_\alpha = \sum_i C_{i,\alpha}\phi_i$, and S is the overlap matrix. When the orbitals are normalized such that the diagonal elements of the overlap matrix are 1, then the off-diagonal elements between the neighboring sites are typically ~ 0.3.[2] Our analysis shows that the overlap matrix does not play an important role, and the results that we present below turn out to be insensitive to such deviation from orthonormality. Therefore, we will take S to be the unit matrix (*e.g.*, $S_{ii} = 1, S_{ij} = 0$ for $i \neq j$) in the remainder of the analysis.[3]

Reproducing the structures of the orbitals found from the full DFT study (see Fig. 6 of the main text and the next section) is an important criterion for finding the parameters, along with the requirement that the spectra of chains consisting of repeating chemical groups

reproduce those obtained by DFT methods. We match the parameters of the TB chain to those orbital structures without considering the oxide layer. However, it should be noted that adding the oxide layer to the model does not change the orbital structures.

We now describe how the tight-binding parameters for the molecules in our papers were determined. In the next section we then discuss how these parameters can reproduce the structure of molecular orbitals.

For the different segments of the molecule we have used the following procedures:

• **Alkane segment and saturated tail group**: The parameters for an alkane chain should satisfy three criteria: (I) From several NEGF calculations,[4,5] it is established that the HOMO is located about 2 eV below the Fermi energy of the metal. (II) The conductance through alkane chains decreases exponentially with molecular length with the exponential rate of $\beta \sim 1$ per methylene group,[4,6–10] i.e. $G(L) = G_0 e^{-\beta L}$. (III) The energy separation between the levels, in particular the frontier orbitals, should be in agreement with that found in DFT. This separation is determined (for a homogeneous chain) by the parameter t, as the levels are distributed according to $E_n - \varepsilon = -2t\cos(k_n a)$ where $k_n = n\pi/L$. Here a is the inter-site distance and L is the effective chain length. From the orbitals found in DFT, we use those that have significant sigma character. The higher energy orbitals are easily identified as such - the lower energy ones tend to hybridize with s-orbitals on the hydrogen atoms. These three criteria together lead to a tunneling parameter $t_{\mathrm{A}} = 6$ eV and a site energy ε_{A} of -14 eV. This value for ε seems very low. However together with the coupling with a value of t about 6, this leads to a level at $\varepsilon + 2t \sim -2$ eV for a long alkane chain.

Our parameters yield $\beta = 1.1$ per CH_2 unit based on the analytical formula $\beta = \cosh^{-1}(-\frac{E_F-\varepsilon-2t}{2t})$ which follows directly from the independent-electron Schrödinger equation.

• **Amide group**: We have performed a DFT calculation for an alternating $[\mathrm{CH_2} - \mathrm{amide}]_n$ chain (with length $n = 8$). The results reveal that the bandwidth of the amide states is about 2 eV. We get a similar bandwidth in our model for the parameters $t_{\mathrm{amide}} = 1.8$ eV,

$t'_{\text{amide}} = 0.5$ eV, $\varepsilon_{\text{CO}} = -1.3$ eV and $\varepsilon_{\text{N}} = -1.8$ eV, which can also reproduce the structure of the highest occupied orbitals, HOMO, HOMO-1, HOMO-2 and HOMO-3.

• **Conjugated R tail group**: (I) Based on Xu *et al.*,[11] for 1.4 $\mathring{A}$ pi carbon bonds, and the HOMO-LUMO gap of DFT calculations for conjugated groups, we choose the tunneling parameter, $t_R = 4$ eV for this tail group. (II) ε_{R} for a conjugated tail is chosen to be 3.5 eV to reproduce the general structure and arrangement of the orbitals. The deviation from the literature value is due to charge transfer at molecule-metal interface shifting the HOMO down. Moreover, $t'_{\text{R}} = 1$ eV is obtained from DFT calculations of a molecule consisting of an alkane chain connected to a conjugated part such as benzene, and is also in agreement with the one obtained by Benkö *et al.*[12]

• **Thiol group**: We take for the site energy and tunneling amplitude the values $\varepsilon_{\text{S}} = -4.2$ eV and $t_{\text{A}} = 6$ eV to localize the HOMO on its own site and with a small weight on the amide group.

• **Oxide layer**: Both experiments[13] and DFT calculations[13] show that for the oxide layer the bandwidth of the valence band is about 7 eV. The parameters chosen for the top and the bottom of the band of the oxide layer are therefore $\varepsilon_{\text{Ox}_\text{t}} = -4.5$ eV and $\varepsilon_{\text{Ox}_\text{b}} = -11.5$ eV respectively. All sites representative of the oxide layer are coupled to the last site of the tail group by $t_{\text{Ox}} = 0.1$ eV .

The results presented below are valid for a range of values of these parameters- see supporting information for details.

In matching the orbital structure from our TBTM to the DFT results shown in Fig. 6 of the main text and Fig. S3, we have found it sometimes necessary to shift the site energies of the tail group somewhat. To obtain a rough estimate of the variation of the potential ε_{R} of the tail group, we performed DFT calculations for the *isolated tail groups* (i.e, tail groups in gas phase with a single hydrogen instead of the attached alkane chain); see Fig. S1. We then take the resulting variation of the HOMO level as an indication of the variation of the tail group site energy. Our DFT calculations show that the variation of the HOMO

energies is ~ 1 eV both in conjugated and in saturated groups. The fact that this potential varies so little from molecule to molecule is largely responsible for the small variation in the current. It should be noted that the HOMO energy in molecules 8-12 is closer to the Fermi energy of the electrodes than in molecule 13 which is due to their larger number of atoms and consequently broader band.

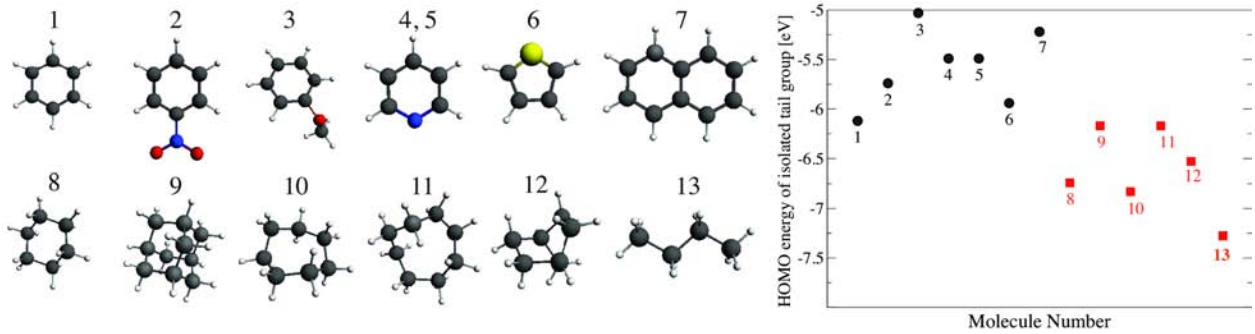

Figure S1: The HOMO energy for the *isolated tail groups* (with a single hydrogen instead of the attached alkane chain). The HOMO energy for the conjugated tail groups (molecules 1-7), is in the range $[-5.05, -6.1]$ eV. The HOMO energy for the aliphatic tail groups in molecules $8-12$ is in the range $[-6.17, -6.8]$ eV.

It may seem impossible to get the HOMO to be localized on the sulphur in view of its ϵ value being lower than that of the amide unit, a difference which would only become more pronounced taking into account the weaker coupling of the amide unit to its neighbours compared with the strong S-C coupling. The reason is that there are *two* orbitals localized on the sulphur, a bonding state, which corresponds to the HOMO-5, and the state which which is anti-bonding with the first C atom, and which forms the HOMO. Also on the amide group, there are two states, one bonding and the other anti-bonding. The weak internal coupling in this group causes the splitting between these two to be quite small, therefore they *both* lie below the HOMO.

Validation of the TBTM Parameters

Using the parameters described in the previous section, we now present the structures of orbitals obtained for our TBTM. Changing the site energy of the tail group (ε_{R}) and its tunneling coupling t_{R} and t'_{R} (see Fig. 7 of the main text) for molecules with conjugated and saturated tails does not influence the HOMO energy located on the thiol linker. To verify this conclusion, we consider the electron population of a few of the highest eigenstates in the TBTM of Fig. 7. For the molecular orbital $\psi_n = \sum_i C_{i,n}\phi_i$, where the sum is over the 17 different sites, the population of site i is $|C_{i,n}|^2$. These populations for the HOMO, HOMO-1, HOMO-2 and HOMO-3 are shown in Fig. S2 for molecules with conjugated ($\varepsilon_{\mathrm{R}} = 3.5$ eV and $t_{\mathrm{R}} = 4$ eV) and saturated ($\varepsilon_{\mathrm{R}} = -14.0$ eV and $t_{\mathrm{R}} = 6$ eV) tails. The structure of the HOMO orbitals is in agreement with our DFT calculations shown in Fig. 6 of the main text and Fig. S3. Furthermore, the lower levels such as HOMO-1, HOMO-2, HOMO-3 of the TBTM are mostly localized on amide (plus tail group in some conjugated molecules), the tail group R or on both. Due to a proper choice of parameters, their structure is in agreement with our DFT calculations.

We now show how the orbitals vary when we alter ε_{R}. We take this variation within 1 eV (as implied by Fig. S1), both for saturated and conjugated tail groups. For molecules with a saturated tail group, shifting the site energy to $\varepsilon_{\mathrm{R}} = -13$ eV does not change the structure of the orbitals, but for molecules with a conjugated tail, shifting the site energy from $\varepsilon_{\mathrm{R}} = 3.5$ to $\varepsilon_{\mathrm{R}} = 4.5$ eV changes the HOMO-2 and HOMO-3 slightly. For $\varepsilon_{\mathrm{R}} = 4.5$ eV, HOMO-2 and HOMO-3 are both distributed over the amide and tail group whereas for $\varepsilon_{\mathrm{R}} = 3.5$ eV, HOMO-2 is on the amide group and HOMO-3 is localized on the R group. These agree well with our DFT results.

Interestingly, the DFT results follow the trend in ionization energies, the methoxybenzene and naphthalene (corresponding to molecules 3 and 7) having the smallest ionization energies of the conjugated group. It may seem surprising that these give the lowest current in figure 5. However, it is important to realize that the HOMO, which is mainly responsible

for the current, only has a very small contribution on the tail group. Therefore, a strong electronegativity on the tail tends to pull the HOMO towards the tail, which increases the transmission. Weaker electronegativity (such as those of tail groups 3 and 7) tends to localize the HOMO more on the sulfur and amide, and this reduces the current, in agreement with the trend seen in figure 5.

These results show that with these selected parameters we can roughly reproduce the structure of the frontier orbitals. The allowed amount of variation for these parameters to reproduce the main features of the orbital structure and current, is about ± 0.3 eV.

Current Obtained Using the Extended Molecule

The details of the coupling between the molecules and the oxide layer are not known – yet the current is quite sensitive to this coupling. In the experiment, the current is the average over a large number of different interface configurations. On the other hand, for both groups of molecules, the sulfur-silver bond is very similar. In our NEGF calculations with gold as the electrode material, we observe a high sensitivity of the current on the molecule-gold configuration. In order to single out the effects of the molecule without the details of the (unknown) interface, we feel that the gas phase results give the most reliable results. For completeness we also present the results for the extended molecule in Fig. S4. Although the results show the same trend as that in Fig. 5, the range of the currents is wider, spanning two orders of magnitude rather than one, due to variations of the tail group-contact interface across the calculations.

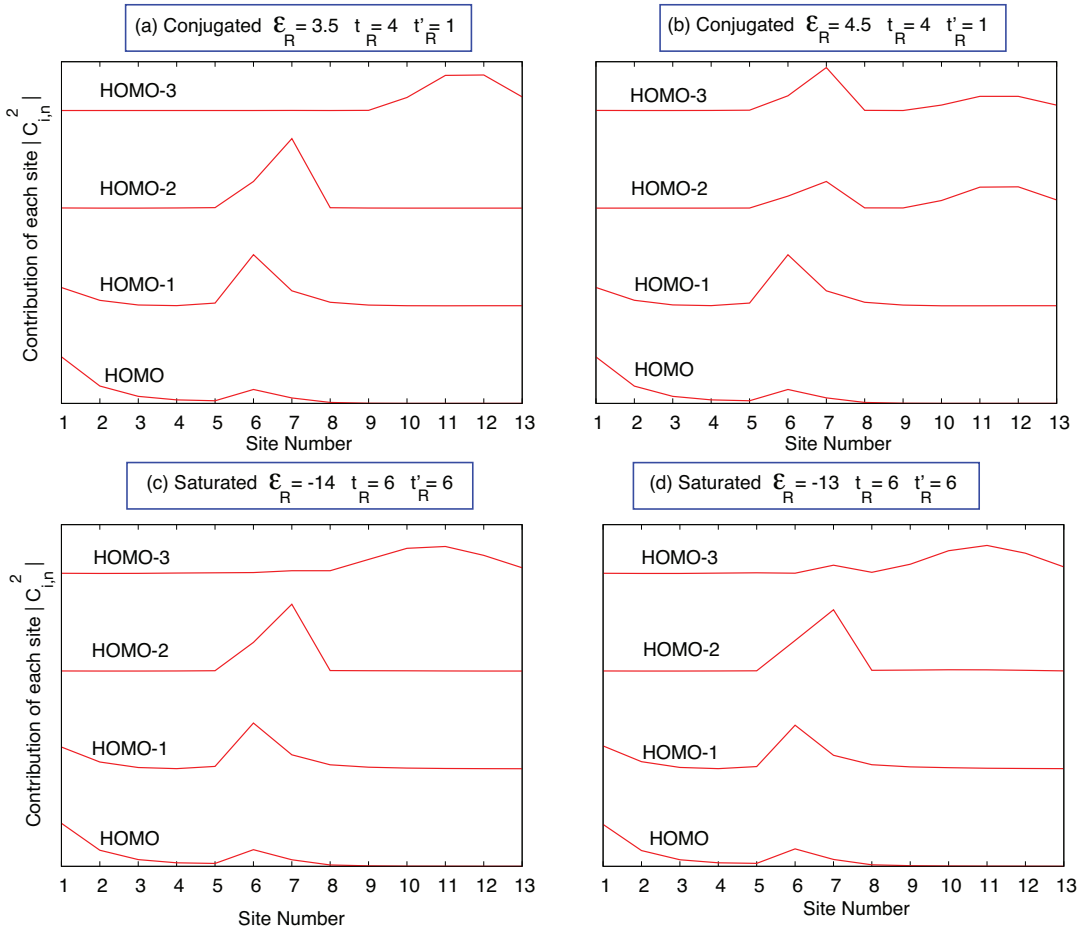

Figure S2: Contribution $|C_{i,n}|^2$ of each site i to the electron population for each orbital n, n = HOMO, HOMO-1, HOMO-2 and HOMO-3 levels. Site 1 is the thiol group and sites 6-7 are the amide group. Sites 10-13 are the tail groups. (a) Molecules with conjugated tail groups $\varepsilon_{\mathrm{R}} = 3.5$ eV, $t_{\mathrm{R}} = 4$ eV and $t'_{\mathrm{R}} = 1$ eV. (b) Molecules with conjugated tail, ε_{R} shifted by 1 eV to see how the variation influences the orbitals. (c) Molecules with saturated tail groups $\varepsilon_{\mathrm{R}} = -14.0$ eV, $t_{\mathrm{R}} = 6$ eV and $t'_{\mathrm{R}} = 6$ eV. (d) Molecules with saturated tail, ε_{R} shifted by 1 eV to see how the variation influences the orbitals. Note that the difference between (a) and (b) for HOMO-2 and HOMO-3 nicely corresponds to Fig. S3.

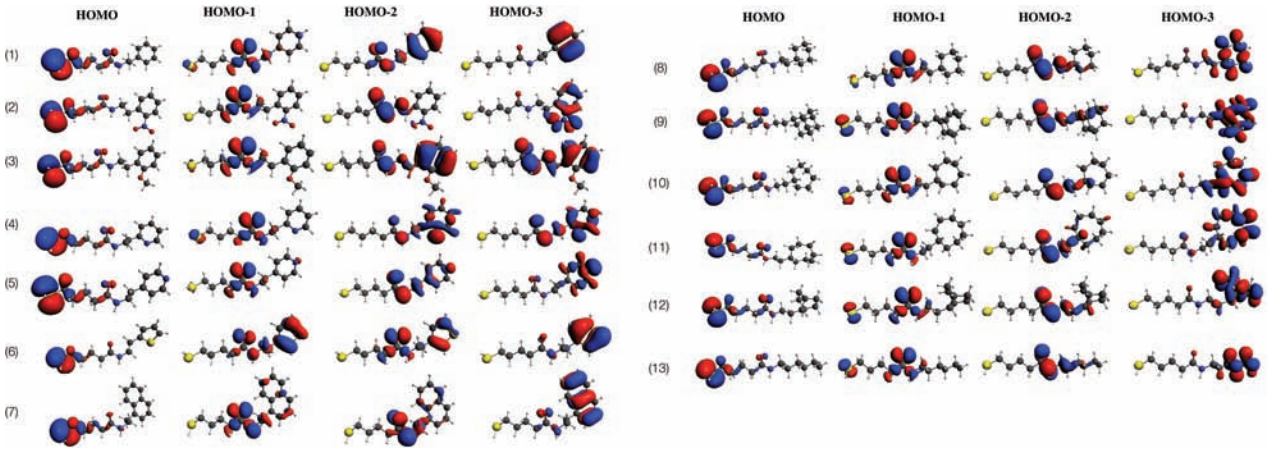

Figure S3: HOMO, HOMO-1, HOMO-2 and HOMO-3 of the molecules 1-13 are mostly located on thiol, amide, amide (plus tail group R), and tail group R respectively. These orbitals are to be compared with their counterparts from the TBTM in Fig. S2. the TMTB indeed mimics the full DFT results very closely.

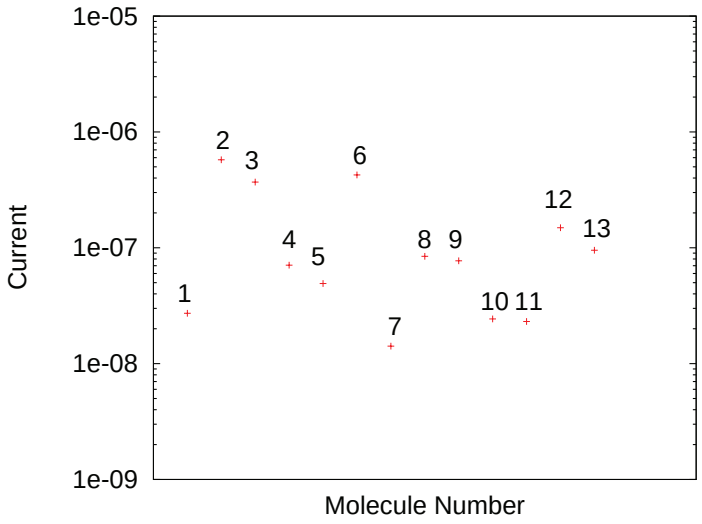

Figure S4: Currents for 0.5 V bias, obtained by integrating the transmission function of the extended molecule.

References

(1) Hoffmann, R. An Extended Hckel Theory. I. Hydrocarbons. *J. Chem. Phys.* **1963**, *39*, 1397–1412.

(2) Mulliken, R. S.; Rieke, C. A.; Orloff, D.; Orloff, H. Formulas and Numerical Tables for Overlap Integrals. *J. Chem. Phys.* **1949**, *17*, 1248–1267.

(3) Jasper, A. W.; Schultz, N. E.; Truhlar, D. G. Transferability of Orthogonal and Nonorthogonal Tight-Binding Models for Aluminum Clusters and Nanoparticles. *J. Chem. Theory Comput.* **2007**, *3*, 210–218.

(4) Li, C.; Pobelov, I.; Wandlowski, T.; Bagrets, A.; Arnold, A.; Evers, F. Charge Transport in Single Au — Alkanedithiol — Au Junctions: Coordination Geometries and Conformational Degrees of Freedom. *J. Am. Chem. Soc.* **2008**, *130*, 318–326.

(5) Cuevas, J. C.; Scheer, E. *Molecular Electronics, an Introduction to Theory and Experiment*; World Scientific, 2010.

(6) Akkerman, H. B.; de Boer, B. Electrical Conduction Through Single Molecules and Self-Assembled Monolayers. *J. Phys: Condens. Matter* **2008**, *20*, 013001.

(7) Lee, T.; Wang, W.; Klemic, J. F.; Zhang, J. J.; Su, J.; Reed, M. A. Comparison of Electronic Transport Characterization Methods for Alkanethiol Self-Assembled Monolayers. *J. Phys. Chem. B.* **2004**, *108*, 8742–8750.

(8) Xu, B.; Tao, N. J. Measurement of Single-Molecule Resistance by Repeated Formation of Molecular Junctions. *Science* **2003**, *301*, 1221–1223.

(9) Slowinski, K.; Chamberlain, R. V.; Miller, C. J.; Majda, M. Through-Bond and Chain-to-Chain Coupling. Two Pathways in Electron Tunneling through Liquid Alkanethiol Monolayers on Mercury Electrodes. *J. Am. Chem. Soc.* **1997**, *119*, 11910–11919.

(10) Smalley, J. F.; Feldberg, S. W.; Chidsey, C. E. D.; Linford, M. R.; Newton, M. D.; Liu, Y.-P. The Kinetics of Electron Transfer Through Ferrocene-Terminated Alkanethiol Monolayers on Gold. *J. Phys. Chem.* **1995**, *99*, 13141–13149.

(11) Xu, C. H.; Wang, C. Z.; Chan, C. T.; Ho, K. M. A Transferable Tight-Binding Potential for Carbon. *J. Physics: Condens. Matter* **1992**, *4*, 6047.

(12) Benkö, G.; Flamm, C.; Stadler, P. F. A Graph-Based Toy Model of Chemistry. *J. Chem. Inf. Comput. Sci.* **2003**, *43*, 1085–1093, PMID: 12870897.

(13) Janowitz, C.; Scherer, V.; Mohamed, M.; Krapf, A.; Dwelk, H.; Manzke, R.; Galazka, Z.; Uecker, R.; Irmscher, K.; Fornari, R. et al. Experimental Electronic Structure of In2O3 and Ga2O3. *New J. Phys.* **2011**, *13*, 085014.